arXiv:1608.08093v1 [physics.atom-ph] 26 Aug 2016

Comment on "Direct photodetachment of F^- by mid-infrared few-cycle femtosecond laser pulses"

G. F. Gribakin* and S. M. K. Law†

Center for Theoretical Atomic, Molecular and Optical Physics,

Queen's University Belfast, Belfast BT7 1NN, United Kingdom

Abstract

Multiphoton detachment of F^- by strong few-cycle laser pulses was studied by Shearer and Monteith using a Keldysh-type approach [Phys. Rev. A **88**, 033415 (2013)]. We believe that this work contained errors in the calculation of the detachment amplitude and photoelectron spectra. We describe the necessary corrections to the theory and show that the results, in particular, the interference features of the photoelectron spectra, appear noticeably different.

* g.gribakin@qub.ac.uk

† slaw08@qub.ac.uk

In Ref. [1] direct photodetachment of F^- by a strong linearly-polarized laser field was considered using the Keldysh-type approach (KTA) [2] generalized to few-cycle pulses [3]. Such methods are useful in general for studying strong-field effects in few-cycle pulses, see, e.g., Ref. [4]. The study was performed for an N-cycle pulse with the vector potential of the form

$$\mathbf{A}(t) = A_0 \hat{\mathbf{z}} \sin^2\left(\frac{\omega t}{2N}\right) \sin(\omega t + \alpha)\,, \tag{1}$$

where A_0 is the peak amplitude, ω is the carrier frequency and α is the carrier-envelope phase (CEP). Photoelectron momentum, angular and energy distributions were generated for a $N = 4$ cycle laser pulse with a range of peak intensities and mid-infrared wavelengths, while examining effects related to above-threshold channel closures and variation of the CEP.

A calculation similar to that of Ref. [1] was also used to identify the effect of electron rescattering in short-pulse multiphoton detachment from F^- computed using the R-matrix with time dependence (RMT) method [5]. Subsequently, an error in the KTA calculations was uncovered [6]. It concerned the phase factors of the contributions to the detachment amplitude that arose from successive saddle points in the KTA calculation for a p-wave electron. Upon correction, the KTA results showed a better agreement with the RMT photoelectron spectra [5, 6]. We believe that the same error affected the results of Ref. [1]. In this comment we show that the interference features of the photoelectron momentum and angular distributions, and the energy spectra are distinctly different from those of Ref. [1] when calculated correctly. We use atomic units throughout, unless stated otherwise.

Using the Keldysh-like approach [2] for the N-cycle pulse (1), one finds the detachment amplitude for an initial state with orbital and magnetic quantum numbers l and m, as (see Eq. (16) of Ref. [1]),

$$A_{\mathbf{p}} = -(2\pi)^{3/2} A \sum_{\mu=1}^{2(N+1)} (\pm)^l Y_{lm}(\hat{\mathbf{p}}_\mu) \frac{\exp[if(t_\mu)]}{\sqrt{-if''(t_\mu)}}, \tag{2}$$

where $\mathbf{p}$ is the final photoelectron momentum and A is the asymptotic normalization constant of the bound electron wave function (for F^- we use $A = 0.7$ [7]). Equation (2) involves a sum over $2(N + 1)$ saddle points t_μ in the complex time plane, $\mathbf{p}_\mu$ and $f(t_\mu)$ being the classical electron momentum and action respectively, evaluated at the saddle points. The terms in the sum in Eq. (2) contain a phase factor $(\pm)^l \equiv (\pm 1)^l$ that alternates (for an odd l) between the contributions from successive saddle points. When the spherical function

$Y_{lm}(\hat{\mathbf{p}}_\mu) \equiv Y_{lm}(\Theta, \varphi)$ in Eq. (2) is evaluated for complex vectors $\mathbf{p}_\mu$, the polar angle Θ is determined by

$$\cos\Theta = \sqrt{1 + p_\perp^2/\kappa_j^2}, \quad \sin\Theta = \mp i p_\perp/\kappa_j, \tag{3}$$

where $p_\perp$ is the component $\mathbf{p}$ perpendicular to the z axis, and $\kappa_j = \sqrt{2|E_j|}$ parameterizes the energy E_j of the bound state for each fine-structure component $j = 3/2,\ 1/2$ of F^- ($l = 1$). The sign in $\sin\Theta$ alternates in the opposite way to ($\pm$) in Eq. (2) and gives rise to an additional m-dependent phase factor. The final expression for the differential detachment probability of an electron from the state l, m reads

$$\frac{dw_{lm}^{(j)}}{d^3\mathbf{p}} = \frac{A^2}{4\pi}(2l+1)\frac{(l-|m|)!}{(l+|m|)!}\left|P_l^{|m|}\left(\sqrt{1+p_\perp^2/\kappa_j^2}\right)\right|^2 \left|\sum_{\mu=1}^{2(N+1)} (\pm)^{l+m}\frac{\exp[if(t_\mu)]}{\sqrt{-if''(t_\mu)}}\right|^2, \tag{4}$$

where $P_l^{|m|}$ is the associated Legendre function. The superscript j is introduced into expression (4) to indicate the detachment from the spin-orbit sublevel j of the ion, which contributes with the statistical factor $(2j+1)/(2l+1)$ to the total detachment probability. The numerical values of κ_j for each fine-structure state of F^- are $\kappa_{3/2} = 0.4998$ and $\kappa_{1/2} = 0.5035$ (using the electron affinity of F^- from Ref. [8]). Note that Eq. (4) takes a similar form to Eq. (33) from Ref. [2] in the case of the long periodic pulse.

The photoelectron momentum densities are axially symmetric and can be obtained from Eq. (4) by taking $\mathbf{p}$ in the Cartesian momentum plane (p_x, p_z),

$$\sum_j \frac{2j+1}{2l+1}\sum_{m=-l}^{l}\frac{dw_{lm}^{(j)}}{d^3\mathbf{p}}. \tag{5}$$

The photoelectron angular distribution is obtained by integrating Eq. (4) over the electron energy $E_e = p^2/2$,

$$\frac{dw}{d\theta} = 2\pi\sin\theta\sum_j\sum_{m=-l}^{l}\frac{2j+1}{2l+1}\int_0^\infty \frac{dw_{lm}^{(j)}}{d^3\mathbf{p}}dE_e, \tag{6}$$

where θ is the polar angle. The photoelectron energy spectrum is given by

$$\frac{dw}{dE_e} = 2\pi\sum_j\sum_{m=-l}^{l}\frac{2j+1}{2l+1}\int_0^\pi \frac{dw_{lm}^{(j)}}{d^3\mathbf{p}}\sin\theta d\theta, \tag{7}$$

and the total detachment probability is

$$w = \int_0^\infty \frac{dw}{dE_e}dE_e \equiv \int_0^\pi \frac{dw}{d\theta}d\theta. \tag{8}$$

In Ref. [5] and, we believe, in Ref. [1] too, the presence of the phase factor $(\pm)^{l+m}$ in the sum over the saddle points in Eq. (4) was overlooked in the calculations. As a result, the detachment probability for p electrons ($l = 1$) was computed correctly for $m = \pm 1$, but incorrectly for $m = 0$, with the interference contributions between the odd and even saddle points added with the wrong sign. Since $m = 0$ electron states give a dominant contribution to the detachment signal, this error affected the interference patterns of the photoelectron momentum and energy distributions presented in Ref. [1] (see [5] and erratum [6]). In addition, we have found that the magnitudes of the photoelectron angular and energy spectra in Figs. 4–7 of Ref. [1] are incorrect. This is in part due to the extra spin factor 2 in Eq. (19) of Ref. [1], which was erroneously retained when accounting for the fine-structure splitting in Eq. (23) of Ref. [1], and also affected the KTA results in Ref. [5]. The purpose of this Comment is to present correct photoelectron distributions for the same wavelengths and other laser-pulse parameters as used originally in Ref. [1].

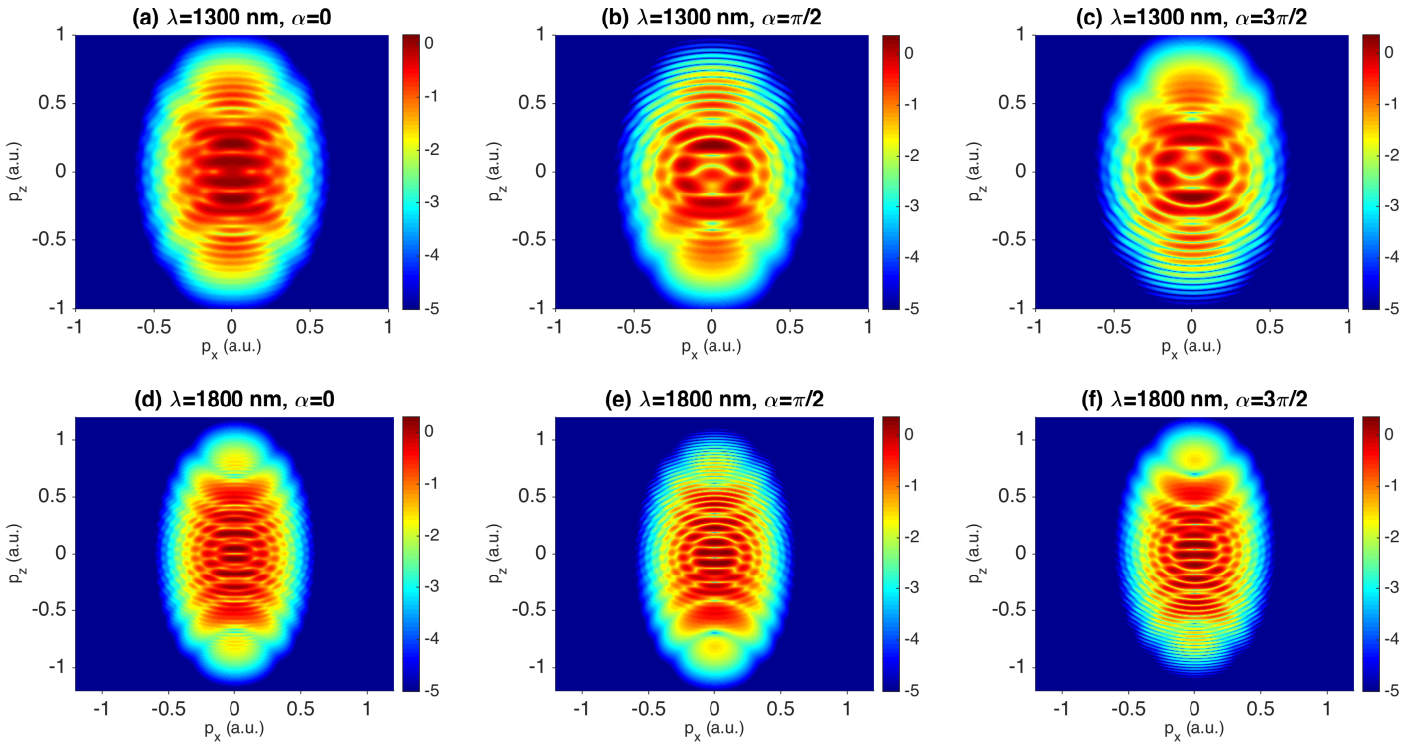

FIG. 1. (Color online) Logarithmic momentum densities for photodetachment of F^- by a four-cycle laser pulse with peak intensity of 1.3×10^{13} W/cm^2. The top and bottom rows corresponds to $\lambda = 1300$ and 1800 nm, respectively, calculated for $\alpha = 0$ [(a) and (d)], $\alpha = \pi/2$ [(b) and (e)] and $\alpha = 3\pi/2$ [(c) and (f)].

Figure 1 displays logarithmic photoelectron momentum densities for photodetachment of F^- by a four-cycle pulse with peak intensity of 1.3×10^{13} W/cm^2 and carrier wavelength of 1300 and 1800 nm, for CEP values $\alpha = 0$, $\pi/2$, and $3\pi/2$. Compared with Fig. 2 of Ref. [1], the correct interference patterns appear more diffuse, lacking any sharp features. Figures 1 (a) and (d) show closer agreement with the momentum densities predicted by the RMT method [5]. At the same time, the overall forward-backward asymmetry along the p_z direction (for $\alpha = \pi/2$ and $3\pi/2$) is generally unaffected, since this characteristic depends on the symmetry of the laser field only.

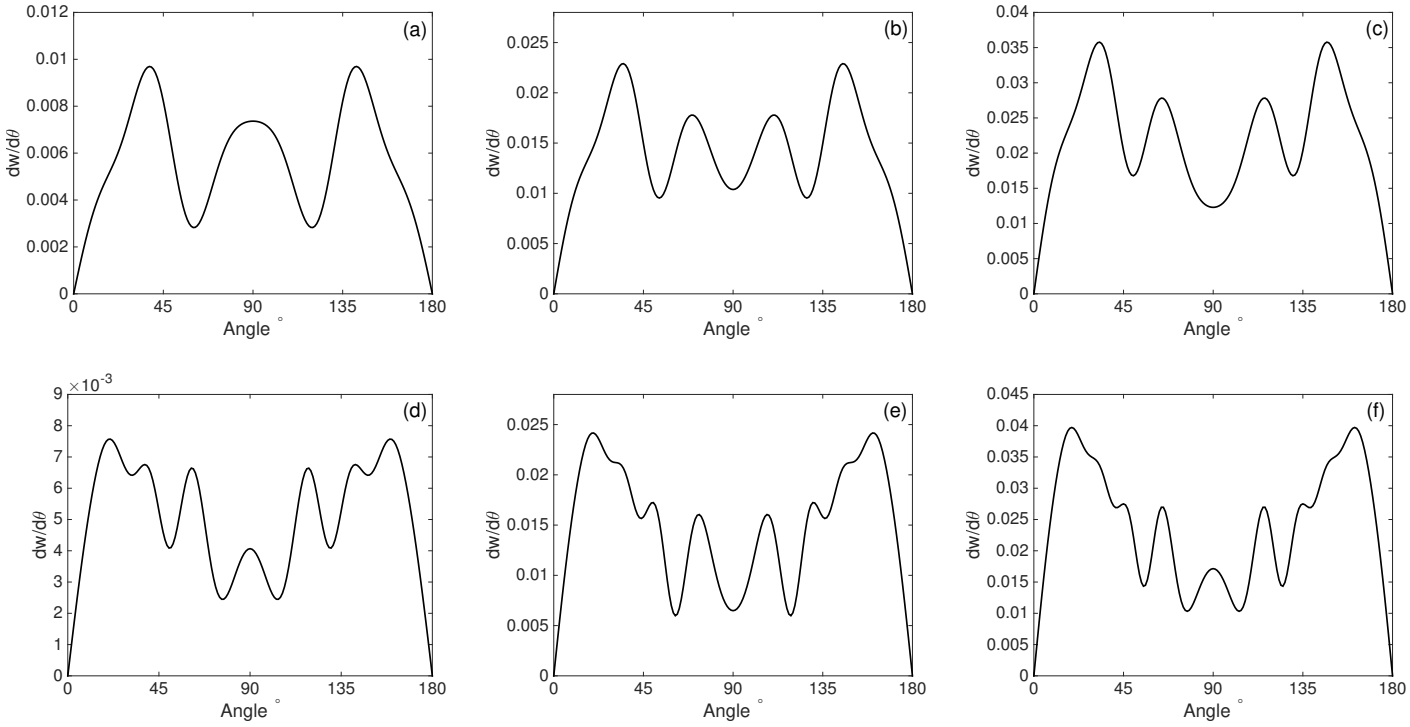

FIG. 2. Photoelectron angular distributions for F^- for a four-cycle pulse with $\lambda = 1300$ (top row) and 1800 nm (bottom row), CEP α=0, and peak intensities 7.7×10^{12}, 1.1×10^{13}, and 1.3×10^{13} W/cm^2 (left, central, and right columns respectively); (a)–(c) correspond to $n_{\min} = 5$, 6, and 6, and (d)–(f) to $n_{\min} = 9$, 10, and 11-photon detachment, respectively.

Figure 2 shows photoelectron angular distributions for F^- for a four-cycle pulse with CEP $\alpha = 0$, wavelengths 1300 and 1800 nm and intensities of 7.7×10^{12}, 1.1×10^{13} and 1.3×10^{13} W/cm^2. Because of the errors mentioned earlier, these angular distributions are very different, both in shape and magnitude, from the (incorrect) results in Fig. 5 of Ref. [1]. The oscillatory structure of the distributions is related to the minimum number of photons

that needs to be absorbed near the peak of the pulse, $n_{\rm min}$ (determined by the integer part of $(U_{\mathbf{p}} + |E_j|)/\omega + 1$ for a given ponderomotive energy $U_{\mathbf{p}} = A_0^2/4$). Analysis of Fig. 2 shows that the angular distributions are characterized by a local maximum (minimum) in the direction perpendicular to the field ($\theta = \pi/2$) when $n_{\rm min}$ is odd (even). This can be seen in Fig. 2 (a), (d) and (f) corresponding to $n_{\rm min} = 5$, 9 and 11, respectively, and in contrast to the original (incorrect) results of [1] where a central minimum for odd $n_{\rm min}$ was noted. The effect of channel closure with increasing intensity gives rise to even $n_{\rm min}$=6, 6 and 10 and a minimum at $\theta = \pi/2$, as seen in Fig. 2 (b), (c), and (e), respectively. This behaviour is in agreement with the observation that for a long periodic pulse the n-photon detachment rate is exactly zero at $\theta = \pi/2$ for odd $n + l + m$ [2], and the fact that $m = 0$ dominates the photoelectron spectrum. Figure 2 also indicates that electron emission at angles close to the direction of the field (i.e., within $0 \leq \theta \leq 45^\circ$ and $135^\circ \leq \theta \leq 180^\circ$) is much stronger here in comparison to Ref. [1], and in better accord with the momentum maps in Fig. 1.

Figure 3 displays the angular distributions computed for CEP values $\alpha = \pi/2$ and $3\pi/2$, and corrects Fig. 6 or Ref. [1]. While the shapes are very different, the degree of asymmetry on the angular distributions for these CEP values is consistent with that seen in Ref. [1].

Figure 4 presents the photoelectron energy spectra for a four-cycle pulse with $\alpha = 0$ and the same wavelengths and intensities as in Fig. 2. It also shows the spectra obtained by including only 2, 3 or 4 saddle points closest to the centre of the pulse. Comparing with Fig. 7 of Ref. [1], we see that the shapes and magnitudes of the correct spectra are quite different from those reported in Ref. [1]. We note that the spectra shown in Fig. 4 (c) and (f) (corresponding to intensity 1.3×10^{13} W/cm^2 and wavelength 1300 and 1800 nm, respectively) show better agreement with those calculated using RMT [5] in the low-energy region (see Fig. 2(c) and (d) of [6]).

For completeness, Table I gives the total detachment probability for F^- for all wavelengths and intensities considered, with CEP values α=0 and $\pi/2$ ($\alpha = 3\pi/2$ and $\pi/2$ give equivalent results). As shown above, correct phases of the terms in the amplitude are crucial for the shapes of the photoelectron momentum, angular and energy distributions. However, they play a relatively small role in the total detachment probability. We have checked that if the latter is calculated by omitting the $(\pm)^{l+m}$ factor in Eq. (4), the total detachment probability

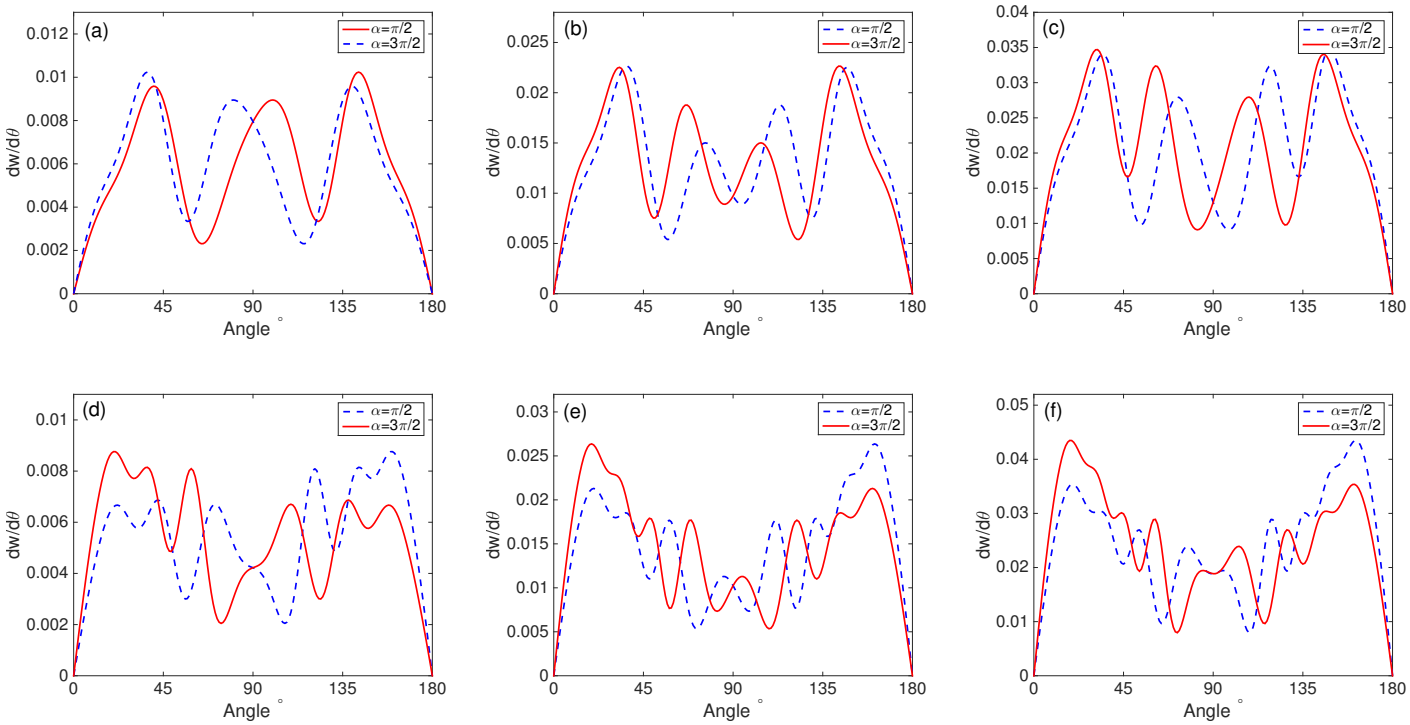

FIG. 3. (Color online) Angular distributions as in Fig. 2 but for $\alpha = \pi/2$ (dashed) and $3\pi/2$ (solid).

TABLE I. Total detachment probabilities for photodetachment of F^- calculated for a four-cycle pulse at wavelengths 1300 and 1800 nm, and different peak intensities I and CEP phases $\alpha = 0$ and $\pi/2$. The last column shows the detachment probabilities per period for a long pulse.

λ (nm)	I (W/cm^2)	$n_{\min}$	w ($\alpha = 0$)	w ($\alpha = \pi/2$)	$w_{\text{no-int}}$[a]	$dw/dt(2\pi/\omega)$
1300	7.7×10^{12}	5	0.0178	0.0185	0.0174	0.0181
	1.1×10^{13}	6	0.0443	0.0412	0.0448	0.0416
	1.3×10^{13}	6	0.0687	0.0659	0.0683	0.0753
1800	7.7×10^{12}	9	0.0159	0.0170	0.0165	0.0165
	1.1×10^{13}	10	0.0468	0.0461	0.0475	0.0497
	1.3×10^{13}	11	0.0752	0.0768	0.0754	0.0789

[a] Obtained by adding modulus-squared contributions from each saddle point in Eq. (4).

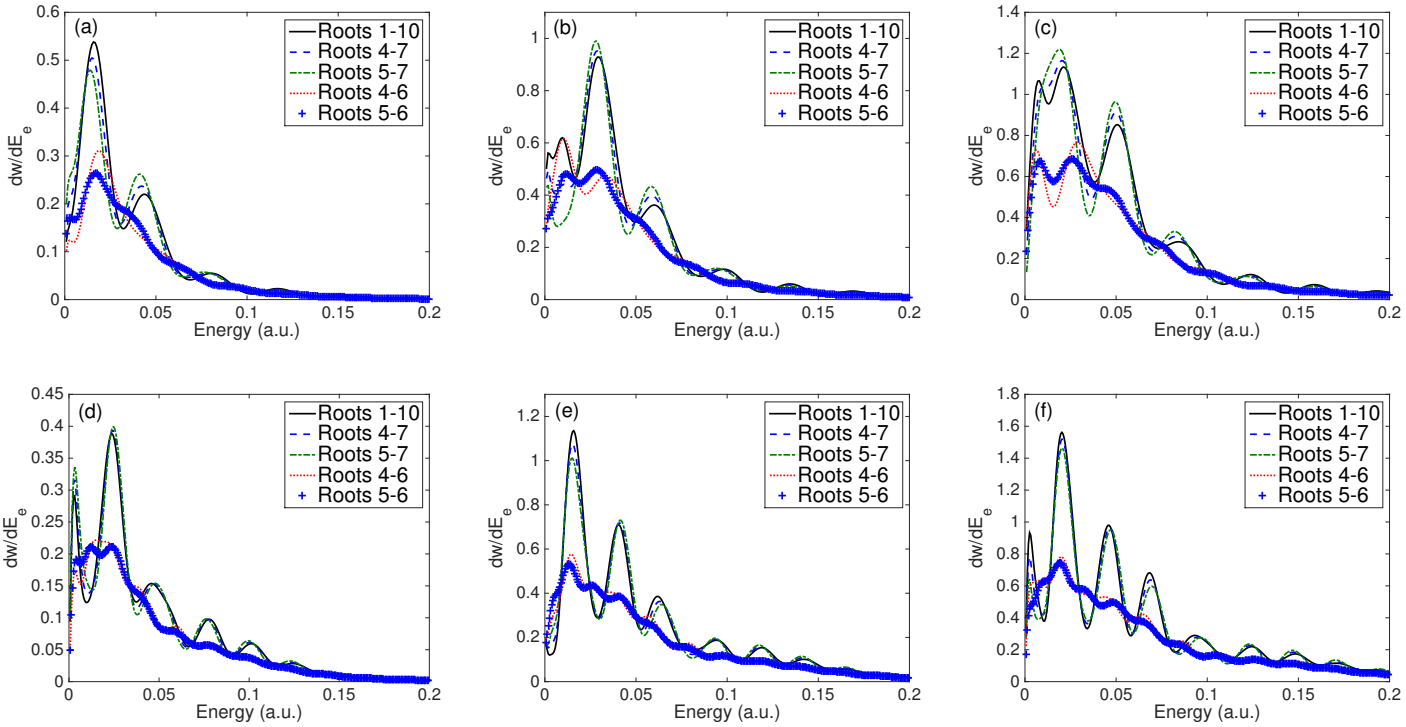

FIG. 4. (Color online) Photoelectron energy spectra of F^- for the same laser pulse parameters for each panel as in Fig. 2. Partial contributions from selected saddle points ("roots") are also shown.

is within 1-2% of the values given in Table I. In fact, the total detachment probability obtained by neglecting the interference terms [i.e., by adding the modulus-squared values of the individual saddle-point contributions in Eq. (4)], $w_{\text{no-int}}$, is within few per cent of the correct value. This shows that the interference of the photoelectron wave packets produced at different laser-field maxima does not lead to much suppression of enhancement of electron emission, but only to some spatial redistribution of the photoelectron flux. The values of $w_{\text{no-int}}$ shown in the second last column of Table I are also practically independent of the CEP (with differences $\sim 0.01\%$).

Shown in the last column of Table I are the detachment probabilities *per period* determined from the KTA detachment rates in a long periodic pulse, dw/dt [2]. They are close to the detachment probabilities in the four-cycle pulse, which implies that effectively, the detachment in the four-cycle pulse is dominated by the central, strongest-field cycle. A similar agreement was seen in Ref. [3] (Table II) which compared detachment probabilities of H^- in a five-cycle pulse with the corresponding one-period long-pulse probabilities from Ref. [2].

Additionally, it is interesting to note that the total detachment probabilities in the short pulse are slightly greater for $\alpha = \pi/2$ than for $\alpha = 0$ if $n_{\rm min}$ is odd, but slightly smaller when $n_{\rm min}$ is even. This effect is entirely due to intereference. It can be explained by the fact that for $\alpha = \pi/2$ the time-dependent electric field $\mathbf{E}(t) = -d\mathbf{A}/dt$ acquires its maximum peak magnitude twice within two central half-cycles, whereas for $\alpha = 0$ the field reaches its peak value once at the middle of the pulse. By comparing the angular distributions (Figs. 2 and 3) for odd and even $n_{\rm min}$ we see that for $\alpha = \pi/2$, constructive interference is more prominent for odd $n_{\rm min}$ near the $\theta = \pi/2$ direction relative to the field, while for even $n_{\rm min}$, destructive interference is more pronounced for angles near $\theta = \pi/2$. This gives slightly higher (lower) total detachment probabilities seen in Table I for $\alpha = \pi/2$ when $n_{\rm min}$ is odd (even).

In conclusion, the photoelectron spectra presented in Ref. [1] were incorrect, in part due to the omission of the m-dependent phase factor in the sum over the saddle points that gives the amplitude. Using the correct phase factor is crucial for obtaining correct interference features of the photoelectron momentum and angular distributions.

ACKNOWLEDGMENTS

We thank H. W. van der Hart and A. C. Brown for useful discussions. S. M. K. Law acknowledges funding from a DEL-NI studentship.

[1] S. F. C. Shearer and M. R. Monteith, Phys. Rev. A **88**, 033415 (2013).

[2] G. F. Gribakin and M. Yu. Kuchiev, Phys. Rev. A **55**, 3760 (1997).

[3] S. F. C. Shearer, M. C. Smyth and G. F. Gribakin, Phys. Rev. A **84**, 033409 (2011).

[4] D. B. Milosevic, G. G. Paulus, D. Bauer and W. Becker, J. Phys. B: At. Mol. Opt. Phys. **39** R203-R262 (2006).

[5] O. Hassouneh, S. Law, S. F. C. Shearer, A. C. Brown, and H. W. van der Hart, Phys. Rev. A **91**, 031404(R) (2015).

[6] O. Hassouneh, S. M. K. Law, S. F. C. Shearer, A. C. Brown, and H. W. van der Hart, Phys. Rev. A **93**, 069901(E) (2016).

[7] E. E. Nikitin and B. M. Smirnov, *Atomic and Molecular Processes* (Nauka, Moscow, 1988).

[8] T. Andersen, H. K. Haugen, and H. Hotop, J. Phys. Chem. Ref. Data **28**, 1511 (1999).